Roland Hessert[a], Wilhelm Satzger[a], Alfried Haase[b], Achim Schafmeister[b]
[a] MTU Aero Engines GmbH, Non-destructive Testing, München, Germany
[b] GE Inspection Technologies GmbH, SEIFERT Analytical X-ray, Ahrensburg, Germany

Cooperating twin robots form a new X-ray diffractometer for stress analysis

Dedicated to Professor Eckard Macherauch on the occasion of the 80th anniversary of his birth

X-ray diffraction measurements on large components with complex geometry are needed in industrial applications requiring the non-destructive characterization of the near-surface material condition in terms of residual stresses, work hardening, phase transformation and formation of reaction compounds. Because many regions of interest on these components are not accessible with conventional laboratory or even mobile X-ray diffractometers, a novel center-free diffractometer with two cooperating robots named "Charon XRD" has been developed at MTU Aero Engines.

Two six-axis robots are synchronized using a special optical measuring system to achieve the highest positioning accuracies. This paper describes the actual design and operating mode of Charon XRD, its current and potential functionality, and presents calibration and reference measurements, along with results on aero-engine high-technology components like bladed integrated disks.

Keywords: X-ray diffraction; X-ray diffractometer; Residual stress analysis; Cooperating robots; NDT

1. Introduction

In industrial fields like aircraft engine construction, components must satisfy stringent requirements regarding reliability, weight, performance, cost-effectiveness and lifetime. Therefore, it is crucial to achieve the full potential of the materials employed. From this aspect, component surfaces and subsurface layers are of special interest, considering that they normally show maximum operating loads and therefore are the most likely source of potential failures.

For the non-destructive characterization of near-surface residual stresses and work hardening on various large complex-geometry components that are inaccessible with mobile diffractometers (see e. g. [1–3]), MTU Aero Engines developed its first stationary large X-ray diffractometer 13 years ago [4]. This computer-controlled, spatially freely positionable diffractometer device was conventionally arranged from linear and rotary axes in a center-free arrangement with a variable measuring circle radius. The movements of the 12 axes for positioning the X-ray tube and the detector above the stationary component under measurement offered high reproducibility. In conjunction with tilt-angle dependent absolute value corrections [5] at a possible tilt-angle range of $-45° \le \psi \le +45°$, measuring accuracies were achieved like those obtained from conventional stationary diffractometers [6]. Residual stresses were determined according to the well-known $\sin^2 \psi$ method [7, 8].

MTU used the results obtained with this laboratory-capable diffractometer device predominantly for optimizing and monitoring manufacturing processes, resolving manufacturing deviations, damage analyses and assessment of new production technologies.

To include the results in lifetime analysis as well, non-destructive inspection of the material conditions in the near-surface zone over the lifetime of the component will become necessary (see e. g. [9–11]). Against this background, and because of new production technologies being developed, constantly increasing measuring tasks on large complex components used in engine construction are required, such as in blisk (= bladed integrated disks) technology for aircraft engines. Accordingly, the existing diffractometer at MTU Aero Engines needed replacing with a newly developed, robust, more powerful and production-capable large X-ray diffractometer for surface stress analyses.

The new "Charon XRD" diffractometer was implemented in accordance with MTU's concept in partnership with GE Inspection Technologies and Robo-Technology [12, 13]. The novel diffractometer concept uses two cooperating six-axis robots that position the X-ray tube and the detector in diffraction geometry relative to the component surface. Apart from achieving considerable flexibility regarding the component geometries to be measured, the aim also was to obtain high positioning and measuring accuracies, fast analysis rates, high maintainability, and user friendliness.

2. Design, function and measuring options

The arrangement illustrated in Fig. 1 and Fig. 2 was implemented for Charon XRD after comprehensive feasibility studies on commercially available high-precision robots, their selection and arrangement, measurement concepts for external robot control, determination of the impact of building vibrations and evaluation of a safety procedure. The Charon XRD includes three main subsystems:

Radiation protection cabin. The robot diffractometer is surrounded by a walk-in X-ray protection cabin providing maximum safety standards. Wide doors allow easy access for comfortable loading of large components. During operation the cabin interior can be monitored through windows in the door and with a controllable camera from the control console. To preclude mechanical collisions from uncontrolled robot movements the cabin walls are protected by wide area motion-sensitive scanners. The cabin temperature is held constant within ± 1 °C.

Fig. 1. Operator control stations in front of the closed Charon XRD X-ray protection and safety cabin.

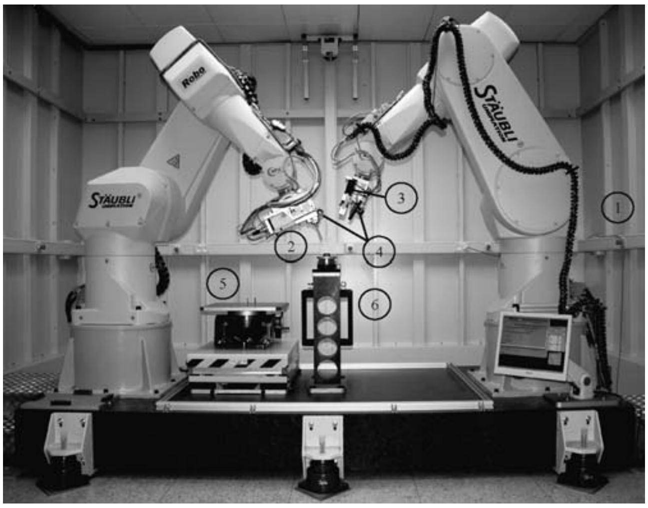

Fig. 2. Interior view of the Charon XRD X-ray robot diffractometer. 1 = radiation protection cabin, 2 = X-ray source, 3 = X-ray detector, 4 = optical measuring system, 5 = component positioning unit, 6 = audit column.

Robot X-ray diffractometer system. The X-ray tube and the detector are each guided by a six-axis RX170B-HP industrial robot from Stäubli. This robot type has a range of 1835 mm and a maximum load capacity of 60 kg with the best presently available spatial positioning accuracy. Each robot moves, referred to its own coordinate system, with an absolute positioning accuracy of ± 0.5 mm when approaching a point and an angular accuracy of $\pm 0.03°$. At constant temperature, its repeatability is about ± 0.04 mm. To improve the precision the bearing play of the robot axes was eliminated by always approaching the desired position from one direction. For technical safety reasons, the robot travel rate was limited to 250 mm s^{-1}.

The two robots are fixed on an elastically supported $3250 \times 1350 \times 300$ mm^3 granite slab to protect against external vibrations. The robots were arranged on the slab in a manner such that, between them, they can accommodate components sized at least $700 \times 700 \times 500$ mm^3 and the optimally measurable volume of $300 \times 300 \times 300$ mm^3 is also located midway between the two robots, 850 mm above the slab.

In order to make stress measurements with diffraction angles 2θ up to 170°, the X-ray source housing and scintillation detector (SD) are each mounted with a corresponding aperture slit system on respective robots in a very compact design. This allowed attachment of optical measuring devices to each side without unnecessary reduction of any beam paths.

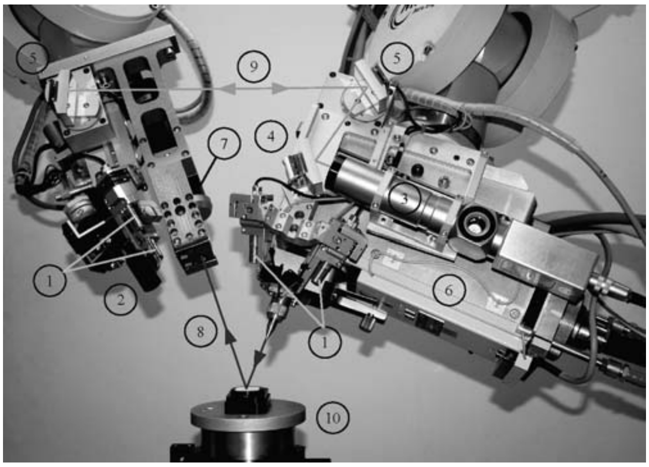

Fig. 3. Detailed view of the optical measuring system to synchronize the two robots. 1= laser line projectors, 2 = camera system, 3 = autocollimation telescope, 4 = fixed deflector mirror, 5 = movable deflector mirror, 6 = X-ray source, 7 = X-ray detector, 8 = X-ray beam, 9 = laser beam, 10 = audit column.

The optical measuring system is an essential part of the new diffractometer and is specially developed (patent pending) to synchronize the two robots. This compact measuring system was optimized so that the angle between the incident and diffracted X-ray beam could permanently be determined within $\pm 0.001°$, and the linear positioning within ± 0.01 mm relative to the component surface in the direction of the bisector of this intermediate angle, in the common coordinate system. Fig. 3 shows details of the optical measuring system.

To control the desired position of the incident and diffracted X-ray beam relative to the component surface, two laser line projectors are mounted on each robot near the X-ray source and the detector. The laser line projectors on each robot are adjusted to each other in such a way that the generated light planes intersect and the sectional line coincides with the X-ray beam direction during diffraction measurements. Accordingly, the intersection of the laser lines on a plane intersecting the light planes marks the position of the X-ray beam. This applies at least to the nominally usable range of the measuring circle radii from 200 to 450 mm, which is determined by the distance of the X-ray tube focus from the measuring point and again by the distance of the measuring point from the detector measuring aperture.

By means of LED illumination and a small industrial CCD camera with a large depth of field, the projected crossed lines from the tube and detector robots and the marked measurement target point on the component (e. g., a colored cross or the light spot of an optical waveguide) are captured and automatically evaluated for a fast iterative position refinement of the two robots until all markers intersect at one point. At a measuring distance of 200 mm, the camera resolution is about 5 µm and the viewing area is about 5×5 mm^2. To position the projected crossed lines of X-ray tube and detector robots at every possible measuring point within the camera viewing area and enable the robots to be precisely positioned, both robots had to be calibrated relative to each other. To describe the movements of each robot in a common coordinate system it was necessary to obtain the transformation matrices from complex optical adjustment and calibration procedures.

The intermediate angle of the X-ray beams is controlled by a laser-based autocollimation telescope, in combination with deflector mirrors mounted on high-precision rotary stages for automatically angle dependent adjustment. Owing to the large intermediate angle range of 10 to 90° ($90° \leq 2\theta \leq 170°$) the wide laser beam issuing from the autocollimation telescope had to be reflected into itself through three precision-adjustable mirrors. This system to determine the intermediate angle simultaneously makes sure that the coplanarity of the incident and diffracted X-ray direction is better than 0.5 mm.

The measuring heads of the tube and detector robot are completely surrounded with so-called “software boxes” to prevent collisions.

Another part of the equipment is an angularly adjustable lift table with air cushion guidance that allows components up to 400 kg in weight to be readily positioned in the diffractometer.

Control and X-ray evaluation software. Standard software is used to control the diffractometer and to evaluate and document measurement results. During operation of the Charon XRD, strict separation is made in the software between the actual diffractometer movements and the transport or alignment movements of the diffractometer itself.

The actual diffractometer movements in step scan mode are comparable with those of a $\theta-\theta$ diffractometer [5] with moving X-ray tube and detector in either focussing Bragg–Brentano or parallel beam arrangement [14]. The measuring circle radii are independently variable between 200 and 450 mm (although for the Bragg–Brentano setup they must be the same size). Determination of the lattice strains can be made at a random azimuth-angle φ ($\varphi \leq 90°$) in the χ-mode [15] with a tilt-angle range of $-70° \leq \psi \leq +70°$ or ω-mode with $-45° \leq \psi \leq +45°$ respectively. Residual stresses are determined using the $\sin^2 \psi$ method.

For surfaces of components inclined up to about $\pm 30°$ relative to the horizontal, the diffractometer can be tilted automatically after a surface normal has been optically determined first. Optimized stress analysis on non-ideal material structures such as coarse-grained materials are possible with special techniques like oscillations at azimuth- and/or tilt-angle movements, along with accumulations of measurements at various component positions. In the presence of strongly curved component surfaces, so-called angle-dependent absolute value corrections can be made. Component surfaces also can be automatically mapped by various techniques.

3. Calibration and reference measurements

To demonstrate the performance and accuracies achieved with the Charon XRD system, various calibration and reference samples were first measured with a high-precision XRD 3003 PTS laboratory system at GE Inspection Technologies in Ahrensburg. Afterwards these samples were measured again on the Charon XRD system at MTU Aero Engines in Munich, using comparable measuring geometries and measuring parameters as far as possible. The measurements were made with characteristic Cu K_α and Cr K_α radiation.

From the measurements on Si powder (SRM 640c) as a standard for calibration of diffraction line positions and line shapes, it was shown that the Charon XRD reproduces with Cu K_α radiation the certified reflection positions over the certified 2θ angular range between 90° and 140° with an error of $\leq 0.01°$ in 2θ.

General verification of the accuracy in the volume of $300 \times 300 \times 300$ mm^3 that can be measured without translation of the sample was made by X-ray diffraction measurements on a single-crystal silicon disk. Owing to its perfect crystal growth, this disk is homogeneous and therefore theoretically provides identical peak positions and profiles everywhere on the surface. More particularly, positioning errors in measuring distance, 2θ angle, or orientation relative to the surface normal must result in relative deviations between the measured peak positions. For this purpose, the disk was tilted in *x*- and *y*-directions (about 30 degrees) and positioned in the center of the measurement volume, see Fig. 4, left. The measured reflections with Cu K_α radiation show very good agreement at all measuring positions in the volume, i. e. peak position, intensity, full width at half maximum (FWHM) and resolution are identical within the measurement statistics, see in Fig. 4, mid and right.

The properties and accuracies of the two diffractometer systems regarding the measurement of near-surface residual stresses were verified using residual stress free Au and Fe reference powders [16]. Typical Charon XRD measurement results from standard Au powder with Cu K_α radiation represented by curves M1 and M2 and from Fe powder with Cr K_α radiation given by curve M3 are shown in Fig. 5.

The results have been obtained with equal measurement and evaluation parameters for residual stress determination. The variation of ψ angles was performed in χ-mode with tilt-angle range from $-70°$ to $+70°$.

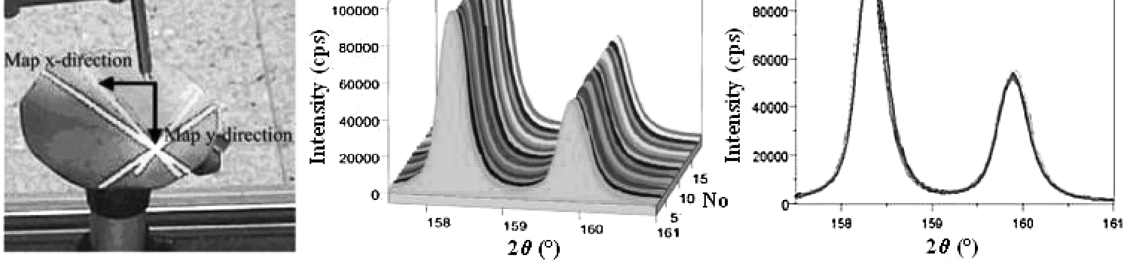

Fig. 4. Setup (left) and intensity profiles in 3D (mid) and 2D (right) of scans in *x*- and *y*-directions on tilted single-crystal silicon disk.

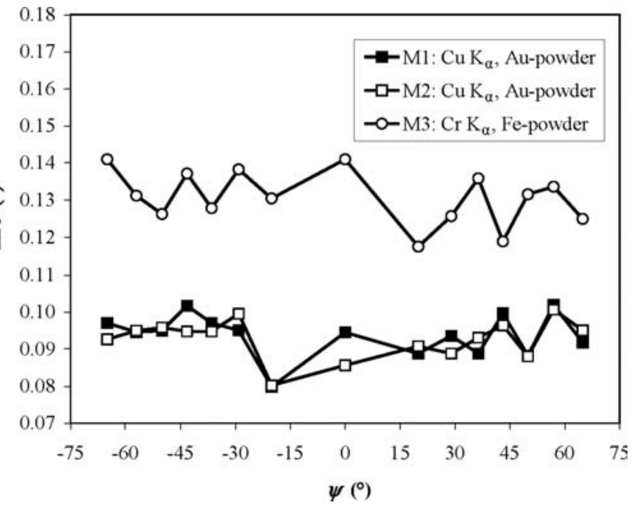

Fig. 5. Accuracy and reproducibility check on stress-free Au and Fe powder with Cu K_α and Cr K_α radiation at Charon XRD. The peak position deviations $\Delta 2\theta$ are plotted against ψ tilt-angles for Au (curves M1 and M2) and for Fe (curve M3) powder.

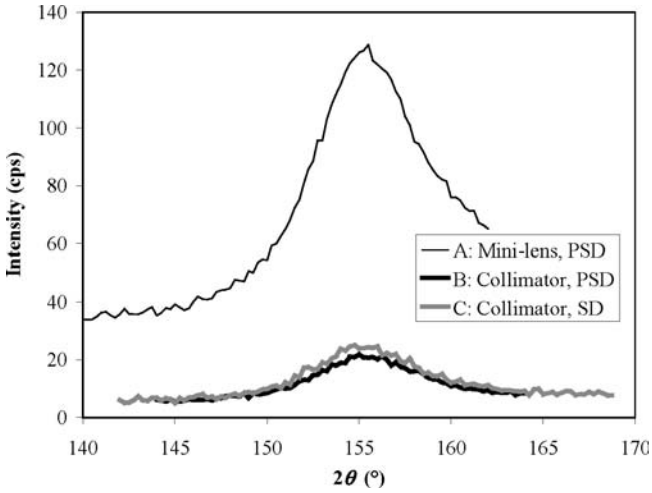

Fig. 6. X-ray diffraction measurements on 100 Cr 6 reference sample (B524) with Cr K_α radiation. Comparison of scans using 1 mm mini-lens primary optic (A) against 1 mm collimator (B) and of peak profiles from SD (C) and PSD (B) with collimator.

The maximum displacement $\Delta 2\theta$ of the calibration peaks from the stress-free powders do not exceed $\pm 0.015°$ in 2θ throughout the total tilt-angle range. The mean deviation of measured 2θ peak positions from the theoretical value of stress-free powder can be used for an absolute line position determination.

Between the two measurements M1 and M2 on Au powder for reproducibility tests both robots were intentionally positioned with high acceleration and extremely wide elongations for several times. The very good agreement of both curves shows a high stability even after extreme endurance testing. The measurement curve M3 proves the stability of the system after easily changing the X-ray tubes from Cu to Cr anode in less than 15 minutes. This is achieved by reproducible adjustment between X-ray focus and collimator system with robust fixation.

The investigation of stressed reference samples was made on ground and shot-peened surface conditions of IN718 and Ti64, both typical aerospace materials. These samples have been measured on various diffractometers and their stress values have accordingly been validated continuously over a period of years. The given measurement data were confirmed within allowable error tolerance [6] through comparative series of measurements on the GE Inspection Technologies high-precision XRD 3003 PTS laboratory system and on the Charon XRD at MTU Aero Engines in Munich.

High precision X-ray diffractograms can be recorded by using automatic optical position control with fine adjustment of Charon XRD before the X-ray measurement on each point will start. By reduction of the number of adjustment control positions the total measurement time can be reduced.

Additional future potentials for faster measurements can be introduced by X-ray optics to increase intensity and by suitable position sensitive detectors (PSD) for wide angular acceptance and highest sensitivity.

With first measurements on the lab system XRD 3003 PTS it was shown that mini-lens optics generate a 6 times higher X-ray spot intensity on the specimen.

The curves in Fig. 6 show a typical example of peak intensities obtained during X-ray measurements on 100 Cr 6 reference sample B524 [17] with compressive stresses introduced by grinding. Obviously the mini-lens gives a 6 times higher intensity.

An additional time reduction is available by using a PSD, because for these broad peaks with 8° FWHM a standard step scan measurement [16] with an SD has to be carried out with 0.8 mm measuring slit and a selected step size of 0.8° (= 8°/10). This results in a 10 times longer total measurement time for the 8° angular range if compared to a PSD measurement with an 8° detector window size.

Using mini-lenses for the primary optics combined with the PSD, allows 60 times faster measurements.

4. Component measurements

To demonstrate the flexibility of Charon XRD, measurements on complex-geometry engine components at positions of interest inaccessible by conventional diffractometers are described below.

For example, non-destructive residual stress measurements in the radial direction at various airfoil positions are necessary to optimize milling operations in blade manufacturing on a compressor blisk of a titanium-base alloy. The setup operation with the projected crossed lines of tube and detector robot to find the ideal component position in the Charon XRD and a typical result from investigations are shown in Fig. 7. Lattice strain analyses were performed with Cu K_α radiation on {213}-lattice planes at 2θ of 140° in the respective achievable tilt-angle range.

For validation of a cast stator of a compressor in a nickel-base alloy, non-destructive surface residual stress measurements in the radial direction at various circumferential positions at different positions on the vibro-polished airfoil surfaces near the blade edge and near the outer and inner shrouds were required. Figure 8 shows the measuring setup and a typical result. Lattice strain analyses were performed with Mn K_α radiation on {311}-lattice planes at 2θ of 151°. Owing to the complex component geometry and the measuring position to be investigated, only a very limited range of tilt-angle ψ could be used.

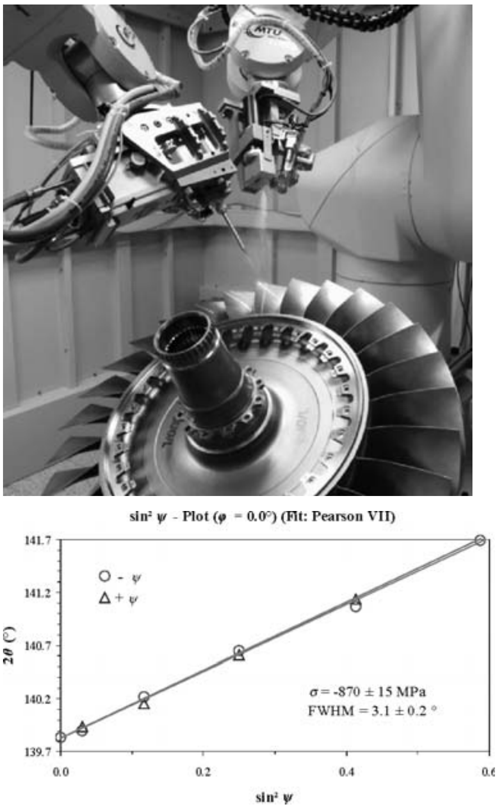

Fig. 7. Setup operation for residual stress measurements on a compressor blisk in the Charon XRD diffractometer (above) and a typical 2θ-$\sin^2\psi$ diagram with the determined results (below) at a measuring position near the blade edge in the blade root region.

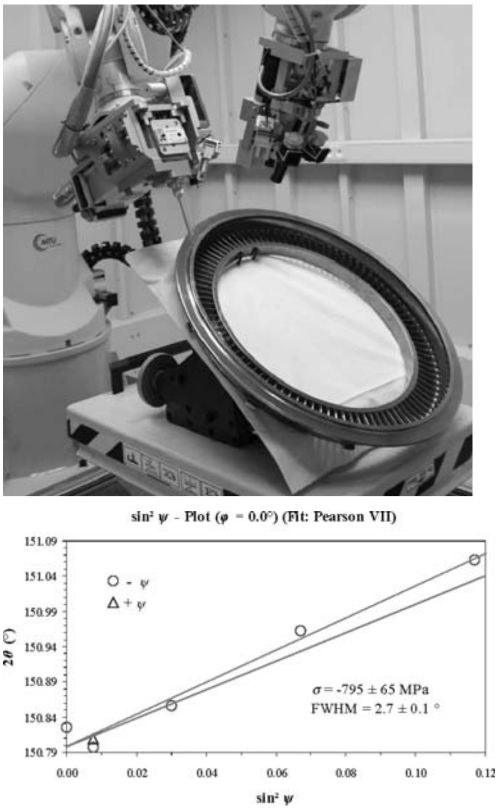

Fig. 8. Residual stress measurement on a stator of a compressor in the Charon XRD diffractometer (above) and a typical 2θ-$\sin^2\psi$ diagram with the determined results (below) at a measuring position near the airfoil edge.

5. Summary

Charon XRD is a center-free large X-ray diffractometer for stress analysis using a novel concept with two cooperating high-precision six-axis robots. The X-ray tube and the detector are each guided by one of the robots. Sufficient positioning accuracy of the two robots relative to one another in a common coordinate system, as required for diffractometer operation, is achieved through a newly developed permanently active optical measuring system providing an absolute angular accuracy of $\pm 0.001°$ and linear positioning in one direction of ± 0.01 mm.

Charon XRD offers a variety of potential configurations, such as upgrade to a PSD or to X-ray optics.

Advantages over current conventional facilities are:

- Maximum flexibility in terms of component geometry, size and variety
- High measuring accuracy in the analysis of residual stress values
- Short analysis times, high maintainability, and user-friendliness.

References

[1] K. Kolb, E. Macherauch: J. Soc. Mater. Sci. Japan 13 (1964) 918.
[2] H. Lange: VDI-Ber. 102 (1966) 51.
[3] V. Hauk, E. Macherauch: Eigenspannungen und Lastspannungen, Beiheft Härterei Techn. Mitteilungen, Hanser-Verlag, München, Wien (1982).
[4] H.U. Baron, E. Bayer, L. Steinhauser, H. Bradaczek, E. Wasiewicz: Europ. J. NDT Vol. 3 No. 1 (1993) 17.
[5] B. Scholtes: Röntgenographische Ermittlung von Spannungen – Ermittlung und Bewertung homogener Spannungszustände in kristallinen, makroskopischen Werkstoffen, Arbeitsgemeinschaft Wärmebehandlung und Werkstofftechnik e. V. Geschäftsstelle, Schlangenbad-Bärstatt (2000).
[6] V. Hauk: Structural and Residual Stress Analysis by Non-destructive Methods, Elsevier, Amsterdam et al. (1997).
[7] E. Macherauch: III. Internat. Kolloquium der Hochschule für Elektrotechnik Ilmenau (1958) 359.
[8] E. Macherauch, P. Müller: Z. angew. Physik 13 (1961) 305.
[9] D. Greving, M. Gorelik, H. Kington, in: D.O. Thompson, D.E. Chimenti (Eds.), Review of Progress in QNDE, Vol. B 24, Plenum, New York (2005) 1339.
[10] S. Vulkelich, S. Berkley, S. Russ, E.F. Bradley: Mat. Evaluation (2002) 884.
[11] R. John, J.M. Larson, D.J. Buchanan, N.E. Ashbaugh, in: A.F. Blom (Ed.), Fatigue, Vol. 2/5, Engineering Materials Advisory Services LTD. (2002) 1063.
[12] MTU Aero Engines Report (winter 2005/spring 2006) 10.
[13] R. Hessert, W. Satzger, A. Haase, A. Schafmeister: Proceedings of ECRS 7, 13–15 September 2006 Berlin, Germany, accepted for publication 16 March 2006.
[14] I.C. Noyan, J.B. Cohen: Residual Stress – Measurement by Diffraction and Interpretation Springer, New York (1987).
[15] U. Wolfstieg: Härterei Techn. Mitteilungen 31 (1976) 19.
[16] European Committee for Standardization, DRAFT prEN 15305: Non-destructive Testing – Test Method for Residual Stress analysis by X-ray Diffraction (July 2005).
[17] V. Hauk: Härterei Techn. Mitteilungen 40 (1985) 232.

(Received April 18, 2006; accepted July 6, 2006)

Correspondence address

Dr.-Ing. Roland Hessert
Non-destructive Testing
MTU Aero Engines GmbH
Dachauer Straße 665, D-80995 München, Germany
Tel.: +49 89 1489 6803
Fax: +49 89 1489 96434
E-mail: Roland.Hessert@muc.mtu.de

You will find the article and additional material by entering the document number MK101374 on our website at www.ijmr.de